Experimental study of a vertical vortex propagating above a smooth wall

Yann Devaux, G. Pineau, D. Calluaud, Lionel Thomas

HAL Id: hal-02140181
https://hal.science/hal-02140181

EXPERIMENTAL STUDY OF A VERTICAL VORTEX PROPAGATING ABOVE A SMOOTH WALL

Y. Devaux[1,c], G.Pineau[1], D. Calluaud[1], L. Thomas[1]

[1]PPrime Institute, 86962 Chasseneuil, France

[c]Corresponding author: Tel.: +0549496979; ; Email: yann.devaux@univ-poitiers.fr

KEYWORDS:

        Main subjects: vortex convection, vertical vortex

        Fluid: water

        Visualization method(s): Particle Image Velocimetry, stereoscopic Particle Image Velocimetry

        Other keywords: isolated vortex, instantaneous flow

ABSTRACT: *This paper proposes an investigation of a vortex propagation over a smooth wall. An isolated vortex is generated experimentally by a pitching plate (chord of 5cm), and propagates along a water channel at a Reynolds of 13000. We focus our study on the near wall region, performing measurements of the flow characteristics with a stereo-PIV technique over five horizontal planes at different heights, and with a PIV technique over one vertical plane. A main vortex can be observed, rotating clockwise, followed by a small secondary vortex with opposite rotation. Those measurements highlight a strong three-dimensional effect, influenced by the characteristics of the pitching plate (maximum angle α_{max} and velocity K_c): a specific pattern with two patches of opposite spanwise velocity is observed, with fluctuations reaching the main flow velocity. The main vortex is columnar at first time steps, and curved itself as it moves forward, convected by the flow: the convection velocity seems to be constant along the streamwise axis, and the main axis of the vortex core does not visibly follow the boundary layer profile.*

1 Introduction

Sediment transport occurs in natural water channels. This equilibrium between soil characteristics and the flow passing above is subtle, and often perturbed by anthropic activities. The scour-hole phenomena, induced by vortices behind a bridge, is a good example: behind a cylinder (modeling a part of a bridge), the flow is subject to a Von Karman vortex street and some horseshoe vortices which erode sediment bed [1].

Some authors studied the influence of turbulence on a sediment bed, artificially increased by grids [2], cylinders [3] or both together [4]: flow perturbations induce a greater transport, which can reach 50 times the original transport (without turbulence added). However, those studies look after a stationary turbulence.

For a better understanding of the contribution of vortices to transport, we choose to study experimentally a vertical eddy in a laboratory water channel. The main idea is to study the convection of an isolated vortex above a sediment bed. Here, we will focus on the hydrodynamic aspects of this study.

Experimental generation of vortices has already been studied. For example, some authors focus on the behaviour of two counter-rotating columnar vortices in a stratified fluid, noticing an hydrodynamic zigzag instability [5,6]. Other investigate the evolution of a columnar vortex in an homogeneous fluid, without any convection [7]. Our experimental apparatus is inspired by those previous works.

Numerical investigations of the flow created by a pitching plate, with a given convection velocity, were proposed, highlighting strong 3D effects and a constant flow structure, for Reynolds numbers from

5000 to 40000 [8] The same case, reproduced experimentally, gives good accordance with those simulations, measuring flow fields by stereoscopic and tomographic Particle Image Velocimetry (PIV) techniques [9,10]. Authors focus on a leading vortex, created along the profile when its angle is already huge (around 40°), and they both highlight a significant spanwise velocity occurring within the vortex; some coherent structure with a filament shape outside of the main eddy can also be noticed [9].

In this paper, we will focus on the tip eddy generated by the pitching movement, on a near-wall region. Using stereo-PIV over 5 different heights, and PIV over a vertical plane, we will look after 3D effects which could potentially affect sediment transport and induce a specific pattern along the sediment bed.

2 Methods

Our experiments were conducted in a water channel at the Pprime Institute (Poitiers, France), using stereo-PIV and PIV techniques. We describe here the experimental setup and the visualization methods used.

2.1 Experimental apparatus

Our water channel is about 6.8m long and 0.39m width, free surface being about h_w=200 mm height, measured by acoustic sensors from Microsonic, with a flow rate of 20 L/s. Front and back walls are made of glass, while PMMA plates (3cm height) are placed above the bottom wall, with a part shaped of black POM (polyoxymethylene) in the visualization area.

The profile, a vertical aluminium plate with a 50mm chord c, 300mm height (exceeding h_w) and 3mm thickness is installed in the median plane of the channel, 2m from the entrance section, disposed in the flow direction. It is rounded on its leading edge and sharpened with a semi angle of 6.5 degrees over 13mm (trailing edge), as represented on Fig. 2.

A stepper motor (HR70C4-44S from SEM) applies to this plate an impulsive move, going quickly to the left side of the water channel at a maximum angle α_{max} with a maximum speed $\dot{\theta}$, before going back at a 0.1 rad/s speed. As some previous studies, our system has a nominal angle of 14° [5]. Fig 1. represents this experimental apparatus.

We can define a Reynolds based on the profile chord, $Re=U_r c/v$, where U_r is the inlet velocity rate and v is the fluid kinematic viscosity. Another non-dimensional parameter K_c can be defined as the tip profile velocity and flow velocity U_r ratio, as used by [9], $K_c=0.9 c\dot{\theta}/U_r$. Temporal variables will be set dimensionless by a time t^*, defined by c/U_r.

In order to characterize our system, measurements were performed over 7 values for α_{max} and 5 values of K_c, as summarized in Table 1.

2.2 Visualization setup

Two set of experiments were conducted, the first one measuring horizontal planes at 5 different heights, with a stereo-PIV technique, the second one vertical planes with a simple PIV technique.

Stereo-PIV: two Dantec SpeedSense 1040 cameras, equiped with 105mm Nikon lenses, were used, providing us 2320x1726 pixels images. To keep a good image quality, Scheimpflug conditions had to be satisfied [11]: specific mounts from LaVision were placed between lenses and cameras, in conjunction with two glass prisms designed with a 30 degree angle (from vertical plane). An horizontal light sheet, 2mm thick, was generated by a Nd-YAG LASER at 532nm. The flow was seeded by 15g of Vestosint particles of a 20µm diameter. This apparatus is presented in Fig 1. Our five planes are

measured from near-wall region (z = 5mm from the bottom wall, as z/c = 0.1) to inner-flow region (z = 50mm from the wall, z/c = 1), with fields of 1.9c (along x axis) over 3c (along y axis).
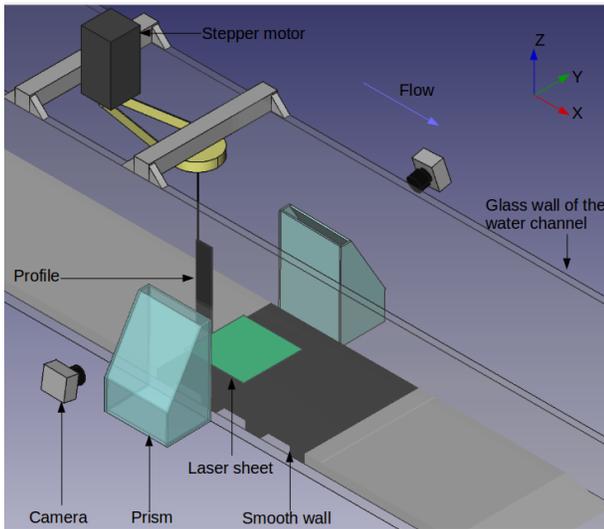

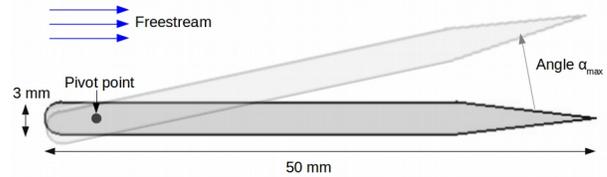**Fig. 1. Experimental setup**

Fig. 2. Profile dimensions

PIV: for those measurements, the LASER was placed above the water channel; a periscope system ("sheet optics for underwater system", from LaVision) brings the Laser beam directly inside the flow, 65cm downstream from the vortex generator (to avoid perturbations). A system of lenses creates a sheet, lightning our profile with an angle $\beta = 12°$ from the median plane: as we will see it in Fig. 5, the vortex path does not follow this median plane during its propagation, so this angle allows us to "cut" the eddy by its middle. Measurement area is about 1.7c along the propagation direction and 2.1c for z axis.

Acquisition system frequency was set to 50 Hz and was managed by Dynamic Studio software. For each case, five runs of 1s are recorded, triggered on the beginning of the profile movement, and one run of 20s, without pitching motion, for flow average information.
Our PIV treatments are made with SLIP Library [12] and consist in multi-passes cross-correlation computation, beginning by 64x64 windows and finishing by 16x16 windows, with an overlap of 50%. For stereo-PIV, a triangulation algorithm computes the third velocity component, resulting in 2D3C fields.

Table 1. Overview of experiments and their parameters.

	α_{max}	K_c	Field of view
stereo-PIV	[8;10;12;14;16;18;20]	[0.1;0.5;1;5;10]	1.9c x 3c
PIV	[10;14;18]	[1;5;10]	1.7c x 2.1c

3 Results

The parametric study performed on our system gives us the vortex behaviour for 5 non-dimensional velocities K_c and 7 angles α_{max}, on 5 horizontal planes (2D3C fields) and one vertical plane (2D2C field), from time $t^* = 0$ to $t^* = 5.1$. A stacked view of the spanwise velocity contours (w'/U_r) over those 2D3C fields is presented in Fig. 3.

The tip of our stationary profile is located at (x/c = 0; y/c = 0). The mean flows $(\bar{u}, \bar{v}, \bar{w})$ - for 2D3C fields - and $(\bar{u}, \bar{w})$ - for 2D2C fields - are calculated and subtracted from instantaneous flows. Therefore, we will focus on velocities fluctuations, identified by $u' = u - \bar{u}, v' = v - \bar{v}, w' = w - \bar{w}$.
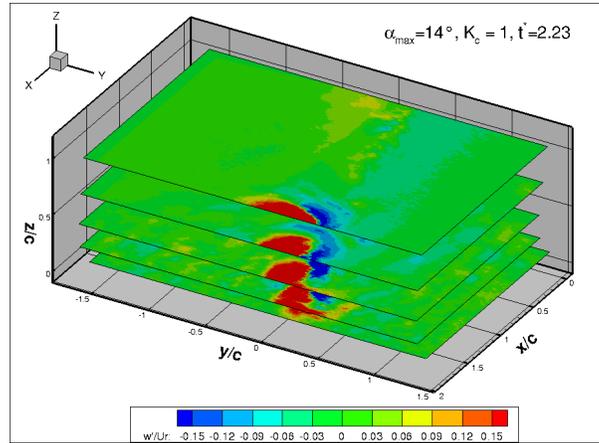

Fig. 3. Fields computed from z/c = 0.1 to 1. Mean field is subtracted and fluctuations of spanwise velocity (w'/U$_r$) are shown

A main vortex is created during the first part of the pitching movement: fluid is expelled by the profile within a region of negative vorticity ω_z. Fig 4 provides an overview of the velocity field fluctuations $(u'/U_r, v'/U_r)$, with a superimposed contour of spanwise velocity w', displaying two areas of different signs. This flow appears to be strongly tridimensional, with w' peaking at U_r. Center of velocity field seems to be located on a positive spanwise velocity area. Those results appear to be coherent with previous studies [9,10].
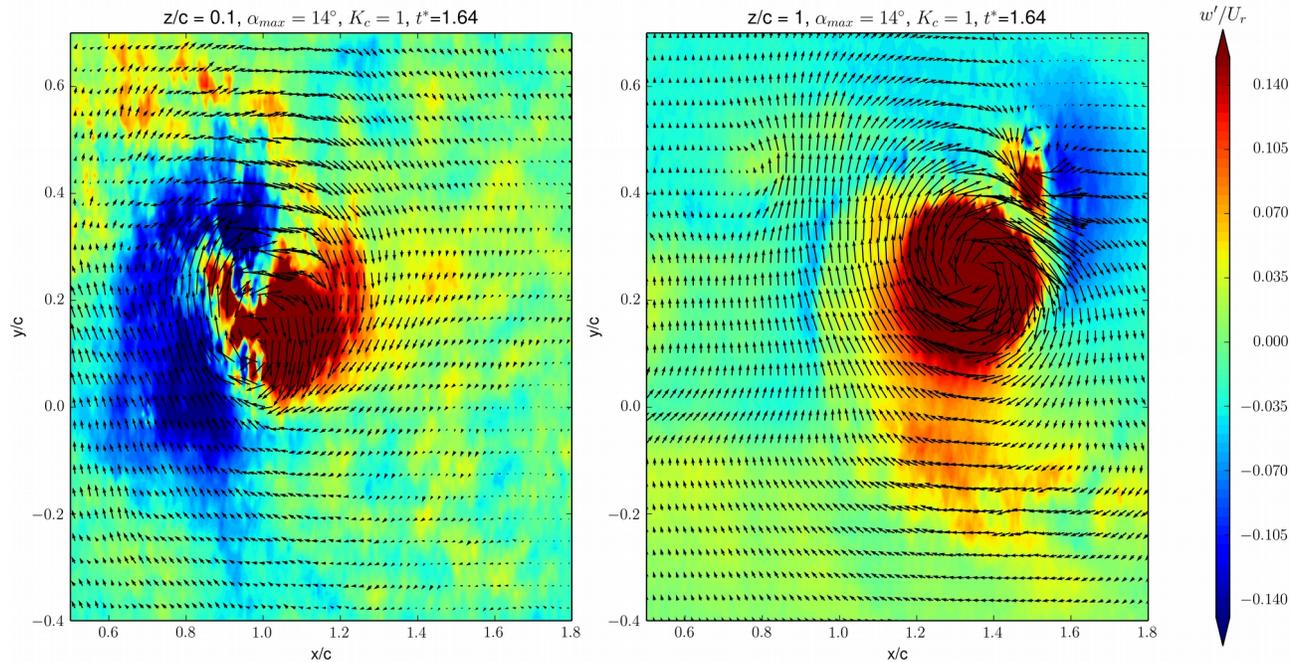

Fig. 4. Velocity field (u'/U$_r$,v'/U$_r$) with spanwise velocity w'/ U$_r$ contour, for z/c = 0.1 (left) and z/c = 1 (right).

A smaller secondary eddy follows the primary one with an opposite vorticity sign and a counter clockwise spin. Those vorticity patterns are well defined in the far-wall region, but as we came closer to the wall, the two patches loose their coherency.

Without any movement, only small vortices are produced and convected in the profile wake by the main flow, at a non-dimensional Strouhal number of St=0.4, where $St = f\,c / U_r$ (the main frequency f being about 2Hz).

Q criterion, introduced by [13], can be used to detect regions where vortices appear and is defined by eq. (1) where S is the strain tensor and Ω the vorticity tensor, defined as eq. (2).

$$Q = \frac{1}{2}\left(\|\Omega\|^2 - \|S\|^2\right) \quad (1)$$

$$S_{ij} = \frac{1}{2}\left(\frac{\partial u_i}{\partial x_j} + \frac{\partial u_j}{\partial x_i}\right), \Omega_{ij} = \frac{1}{2}\left(\frac{\partial u_i}{\partial x_j} - \frac{\partial u_j}{\partial x_i}\right) \quad (2)$$

Here, our first experiments with stereo-PIV show that our vortex path is not linear and does not follow a given x plane: with a detection of vortices centers, we can identify the main axis for the propagation. Fig. 5 presents the tracking made for various angles for horizontal field z/c = 1: we see that a first part is common, before x/c = 0.75, for all angles. This path is about 12° from the median plane, starting at x/c = 0.12 from the tip location. After x/c = 0.75, the followed path seems to depend on α_{max}: as the angle increases, the "reattachement point", where the vortex core falls back to y/c = 0 plane, gets away from the trailing edge.
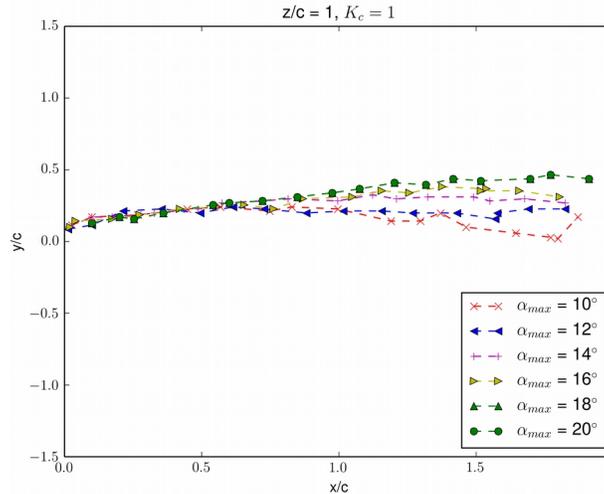

Fig. 5. Vortex centers trajectories for variable angles.
Profile end is initially located at (x/c = 0; y/c = 0).

Comparing the center tracking, as in Fig. 5 for different z/c values, a curved shape can be observed: it can be seen in Fig. 4, as the two regions of positive/negative spanwise velocity are not located at the same coordinates. In fact, near the profile (when x/c = 0), the vortex appears to be columnar, the velocity field produced is homogeneous with respect to the z-axis. The free stream convects this columnar vortex, deforming it in a "tornado-like" shape.

Fig. 6 presents three moments, with the curved profile of the vortex. About this particular tornado shape, 4 parts can be distinguished [14] : outer flow and inflow layer depend on the free stream characteristics, the core is the main part, mostly columnar and the corner is the lower part of the vortex,

curved because of the propagation above a finite wall. The core seems to be 0.5c wide at its maximum for $\alpha_{max} = 14°$ and $K_c = 1$, far from the wall, and we clearly see that this core become less and less coherent as it propagates and fades into the water channel.
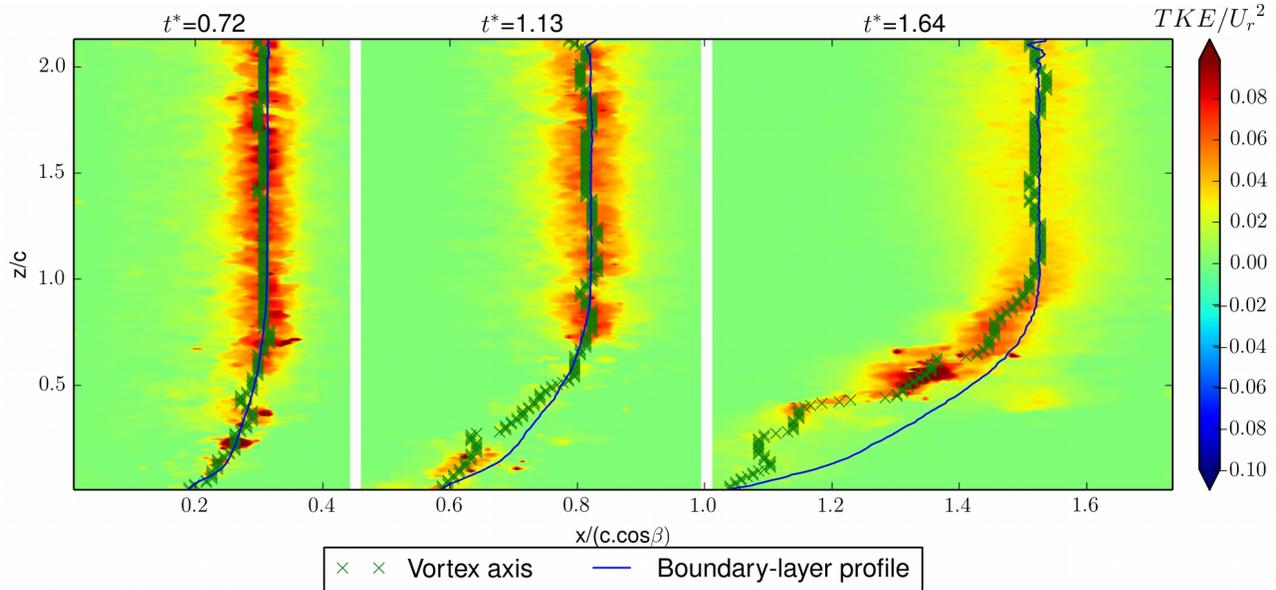

Fig. 6. Visualization of vortex propagation, from left to right (free stream subtracted). Boundary-layer profiles are extracted from a mean field (average of 1000 time steps), vortex axis are detected from u' variations.

As we made a measurement over 1000 time-steps of the stationary flow, we can estimate a mean-flow and the boundary-layer profiles related. Seeking in our instantaneous fields where the corner connects to the smooth wall ($y/c = 0$), boundary-layer are plotted at the same x/c. Here, the eddy structure center seems to follow, in the beginning, the free stream boundary layer.

A convection velocity U_{conv} of the corner can be calculated: for $\alpha_{max} = 14°$ and $K_c = 1$, U_{conv} is about 0.9 U_r. Far from the wall, this velocity is about 1.1. The influence of α_{max} appears to have a small effect: for the former case, a change from 10° to 18° modifies U_{conv} from 0.8 to 0.9 U_r. This convection velocity seems to be constant over the propagation time. Influence of velocity K_c over the vortex formation is presented Fig. 7.

A low velocity ($K_c = 0.1$) creates only a weak eddy, difficult to identify, with w' fluctuations not so far from the mean flow. But, from $K_c = 0.5$, flow perturbations are sufficient to generate a w' peaking to 0.5 U_r near the wall. The winding shape starts to be visible from $K_c = 1$. Note that a similar behaviour can be observed for an angle variation ($\alpha_{max} = 10°$ is a "threshold" for observable fluctuations of spanwise velocity).

The maximum tangential velocity U_θ is mainly influenced by K_c. It peaks at 1.9 U_r for $\alpha_{max} = 14°$ and $K_c = 1$. It seems to grow linearly when maximum angle increases, but variations of K_c seem .
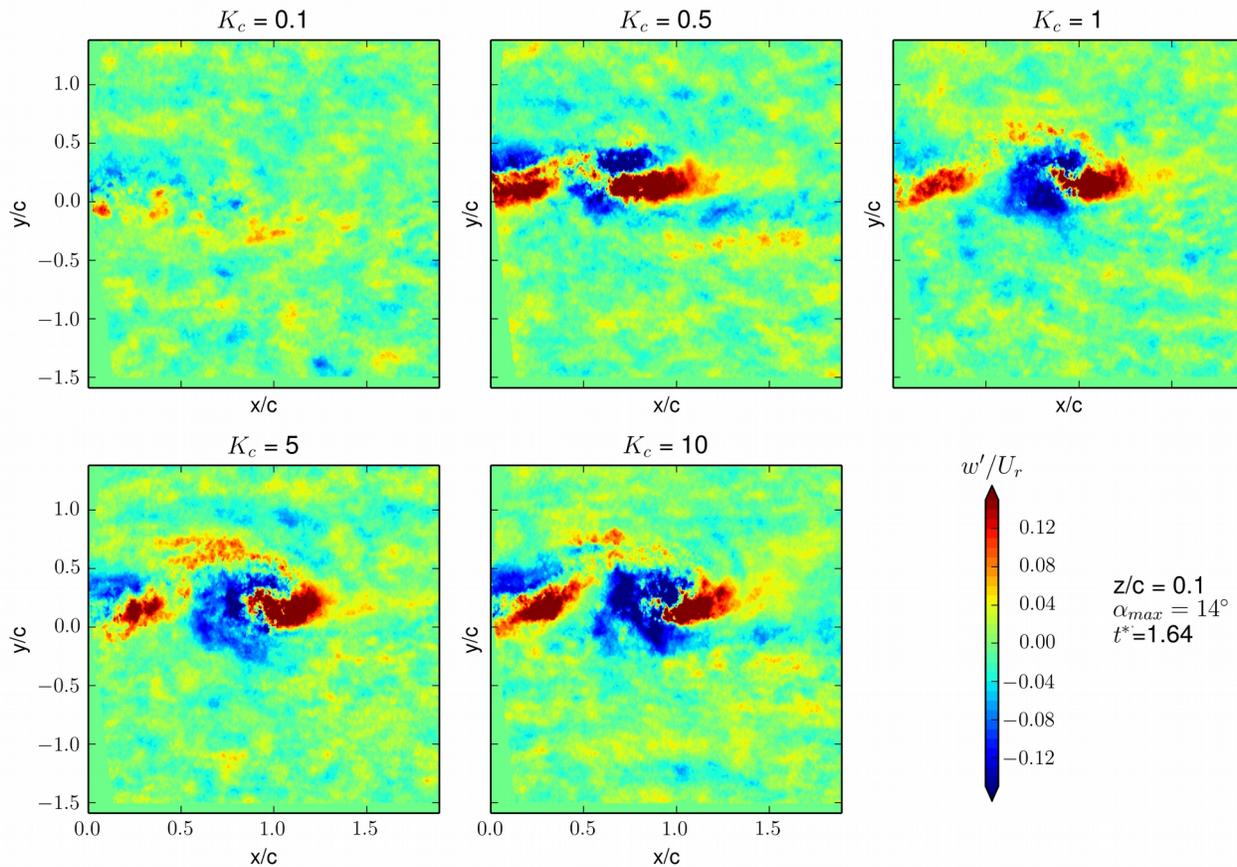
Fig. 7. Variations of spanwise velocity. Each image is phase-averaged with 5 different runs. α_{max} is given, and fields are represented in the near-wall region (z/c = 0.1).

4 Conclusion

This paper examined the instantaneous flow in the wake of a pitching plate moving quickly to a maximal angle α_{max} at a given speed K_c. Boundary conditions are a smooth wall on the bottom and free-surface on the top, with a flow rate corresponding at Reynolds Re = 13000. Measurements are performed with PIV and stereo-PIV, and we focus on the near-wall region. As the fluid is expelled by the moving plate, a region of negative vorticity is generated on all the water height, its center corresponding to an area of positive spanwise velocity. This main vortex region is followed by a smaller secondary one, with an opposite vorticity, which spin around the main eddy during the propagation along the water channel.

For first time-steps, the vortex shape is columnar, but as it is convected, two parts can be distinguished: the core, on the top, which keep a uniform pattern with a convection velocity greater than the average velocity U_r; the lower part, which is moving slower and takes a tornado shape. The profile parameter α_{max} is the main influence of vortex structure, on its maximal tangential velocity, on the maximal fluctuations of spanwise velocity, and on its trajectory. Nevertheless, velocity patterns observed for u',v' remain similar, and a specific winding shape is noticed, with two patches of opposite

sign, for w'. Further measurements, using a tomographic PIV technique, could be useful to investigate more accurately the 3D structure of this vortex.

As vortex structures are known to transport sediment easily, further experiments will be performed with the same apparatus, replacing the smooth wall boundary condition by a sediment bed: specific attention will be payed at the initiation of transport.

References

[**1**]   Hopfinger E J, Kurniawan A, Graf W H and Lemmin U. Sediment erosion by Görtler vortices: the scour-hole problem. *Journal of Fluid Mechanics*, Vol. 520, pp 327–342, 2004.

[**2**]   Okayasu A, Fujii K and Isobe M. Effect of external turbulence on sediment pickup rate. *Coastal Engineering Proceedings*, Vol. 1, 2011.

[**3**]   Cheng N-S. Comparison of sediment pickup rates over plane bed and dunes. *Journal of Hydraulic Engineering*, 2016.

[**4**]   Sumer B M, Chua L H C, Cheng N-S and Fredsøe J. Influence of Turbulence on Bed Load Sediment Transport. *Journal of Hydraulic Engineering*, Vol. 129, pp 585, 2003.

[**5**]   Billant P and Chomaz J. Experimental evidence for a new instability of a vertical columnar vortex pair in a strongly stratified fluid. *Journal of Fluid Mechanics*, Vol. 418, pp 167–188, 2000.

[**6**]   Lacaze L, Brancher P, Eiff O and Labat L. Experimental characterization of the 3D dynamics of a laminar shallow vortex dipole. *Experiments in Fluids*, Vol. 48, pp 225–31, 2009.

[**7**]   Hirsa A, Lopez J M and Kim S. Evolution of an initially columnar vortex terminating normal to a no-slip wall. *Experiments in Fluids*, Vol. 29, pp 309–21, 2000.

[**8**]   Garmann D J and Visbal M R. Numerical investigation of transitional flow over a rapidly pitching plate. *Physics of Fluids*, Vol. 23, pp 094106, 2011.

[**9**]   Buchner A-J, Buchmann N, Kilany K, Atkinson C and Soria J. Stereoscopic and tomographic PIV of a pitching plate. *Experiments in Fluids*, Vol. 52, pp 299–314, 2012.

[**10**] Buchmann N, Buchner A-J, Kilany K, Atkinson C and Soria J. Multi-Component - Multi-Dimensional PIV Measurements for a Flat-Plate Pitching Motion 40th Fluid Dynamics Conference (Chicago, Illinois: American Institute of Aeronautics and Astronautics), 2010.

[**11**] Prasad A K. Stereoscopic particle image velocimetry. *Experiments in Fluids*, Vol. 29, pp 103–16, 2000.

[**12**] Tremblais B, David L, Arrivault D, Dombre J, Thomas L and Chatellier L. *Simple Library of Image Processing (SLIP)*, 2010.

[**13**] Hunt J C R, Wray A A and Moin P. Eddies, streams, and convergence zones in turbulent flows Studying Turbulence Using Numerical Simulation Databases, 2, 1988.

[**14**]   Lewellen W S. Tornado Vortex Theory. *American Geophysical Union Geophysical Monograph Series*, Vol. 79, pp 19–39, 1993.